SUGISAKA MASANORI

Journal of Robotics, Networking and Artificial Life
Vol. 10(2); September (2023), pp. 184–191
ISSN (Online): 2352-6386; ISSN (Print): 2405-9021
https://alife-robotics.org/jrnal.html

Research Article

Robotic Assembly of Gearmotors: Stator Insertion Operation Using Pose Detection and Contact Position Estimation

Takayoshi Yamada[1], Yasumoto Imai[1], Junya Sato[1], Toshiki Hayashi[2], Shota Aono[2]
[1]Department of Mechanical Engineering, Gifu University, Yanagido 1-1, Gifu 501-1193, Japan
[2]Tsubakimoto Chain Co., Nakanoshima 3-3-3, Kita-ku, Osaka 530-0005, Japan

ARTICLE INFO

Article History

Received 11 November 2022
Accepted 25 October 2023

Keywords

Assembly automation
Robot
Gearmotor
Keypoint matching
Contact position estimation
Image sensor
6-axis force torque sensor

ABSTRACT

We discuss a system of robotic assembly for gearmotors which are also called gear motors or geared motors. A gearmotor consists of a reducer, a rotor, a stator, a bracket, bolts, and so on. This paper focuses on an assembly task of the stator to the rotor and reducer. The task is complicated because the fit diameter of the stator and rotor is clearance fit. Currently, the task is performed by manual handwork of skilled workers. To accomplish the task, the workers utilize various information such as visual and hand sensation. We develop assembly system using robots, vision, and force torque sensors to automatize the task. Two main methods, key point matching and contact position estimation, are applied to perform the task. Keypoint matching is utilized to detect the pose (position and orientation) of the stator by using visual information. Contact position estimation is utilized to detect the contact between the parts during the insertion process by using force information and to prevent failure of the insertion operation. The validity of our proposed system is verified using experiments of the automatic insertion task of the stator.

1. Introduction

In production lines, various processes exist in which include machining, assembly, inspection, and so on. In these processes, much manual handwork by skilled workers remains. We aim to automatize the processes by using robots.

Dexterous hands and sensitive senses are inherent in human beings. As a result, the beings are able to handle complicated tasks easily. However, various human error occurs in manual hand work. Mateus et al. [1] and Gervasi et al. [2] discussed Human-Robot collaboration in some of assembly processes. In order to make good use of both strong points of humans and robots, the collaboration arises, in which comparative simple tasks (i.e., handling and positioning) are carried out by robots and comparative complicated tasks (i.e., assembling and screwing) are performed by human workers.

Salunkhe et al. [3] discussed a wheel hub nut assembly system. A truck wheel hub is considered. Since the size of hub and the number of nuts to be mounted are large, it is very cumbersome to mount the nuts to the hub by manual handwork. To automatize the work, the assembly process is improved by using a Cobot (Collaborative robot). Ma et al. [4] tackled a precision assembly system for assembling small parts using microscopic vision and force sensor. Song et al. [5] explored skill learning for robotic assembly. Visual and force information are utilized for the learning. The method is evaluated using a circuit breaker assembly system. Chang [6] tackled robotic assembly of smartphone back shells. Eye-in-hand visual servo is utilized.

Figure 1. Gearmotor

Corresponding author E-mail: yamada.takayoshi.d9@f.gifu-u.ac.jp, sato.junya.c5@f.gifu-u.ac.jp

[Figure 1](#) shows a gearmotor which is also called a gear motor or a geared motor. It is a motor packaged with a reducer connected to a rotating shaft of an AC or DC motor. It is widely used in cranes, conveyers, transport equipment, and so on. The gearmotor consists of a reducer, a stator, a rotor, a bracket, bolts, and so on. In assembly processes of the parts, various assembly tasks must be performed such as gear insertion of the rotor into the reducer, clearance fit insertion of the stator to the rotor, and so on. These tasks are complicated. Currently, gearmotors are assembled manually by skilled workers, in which high level abilities are required such as dexterous and sensitive hands and advanced visual information.

We discuss an automatic insertion method of the stator to the rotor and reducer, in which the rotor is pre-assembled to the reducer beforehand. Section 2 explains an overview of our robotic assembly system in which includes assembly equipment and a hardware configuration. Section 3 explains keypoint matching for orientation detection of the stator by using a vision system and contact position estimation by using a force torque sensor for preventing failures in insertion operations. Section 4 verifies the effectiveness of our proposed robotic assembly system.

2. Overview of the experiment system

Figure 2 shows our experiment system. Denso VS-050 is an articulated robot arm used for parts assembly. Leptrino PFS055YA251 is a 6-axis force torque sensor to acquire contact force and moment measurements. Intel RealSense D435 is an RGB-D camera to capture visual information. Robotiq 2F-140 is a 2-finger robot hand to grasp the parts. The sensor, camera, and hand are mounted on the end of the robot arm. These devices are connected to a computer. The arm is controlled by a C program on the computer via an ORiN2 middleware and an RC8 robot controller. The assembly target is a gearmotor manufactured by Tsubakimoto Chain Co.. Figure 3 shows an assembly environment. The reducer is placed on a jig created by a 3D printer in our laboratory. The rotor is pre-assembled to the reducer beforehand. To enhance the robotic assembly technique like human workers, we suppose that the stator is put on a workbench roughly.

Figure 2. Handling System

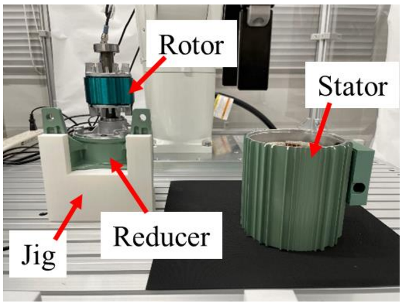

Figure 3. Assembly Environment

3. Assembly motion generation of the stator

The stator is detected by using image recognition of the wrist camera, grasped by the robot hand, and inserted by using contact recognition of the force torque sensor. The robot must make corrective motion appropriately because the fit diameter between the rotor and the stator is clearance fit, detection error of the image recognition arises, and pose (position and orientation) error of the grasping arises. We discuss a generation method of the appropriate motion.

Using the steps shown in Figure 4, the center of the hand is aligned just above the center of the stator. In the process, Hough transform is used for center alignment of the wrist camera and the stator (Figure 5). It is necessary to detect the orientation of the stator for the alignment because the reducer, stator and bracket are fixed using threaded holes and through long screws after the parts assembly. Keypoint matching is used for pose alignment of the hand and the stator.

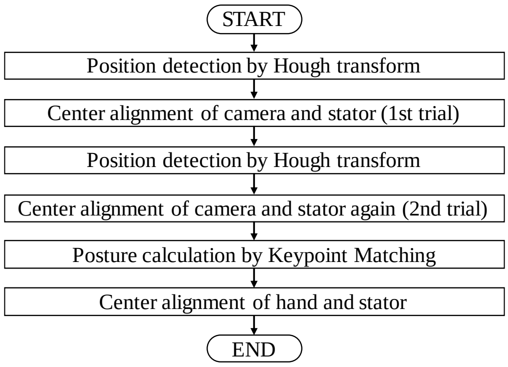

Figure 4. Flowchart of the insertion process

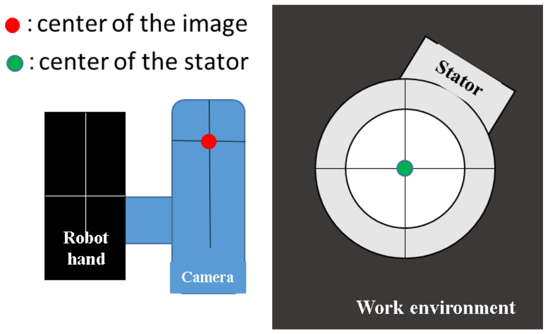

(a) Top view of the setup

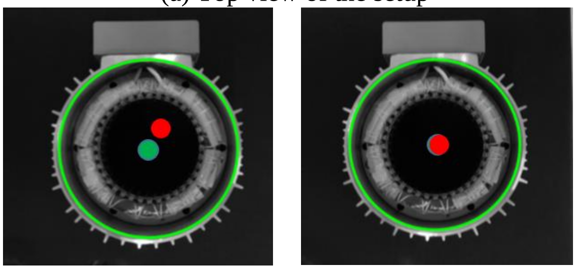

(b) The 1st trial of the center alignment (c) The 2nd trial of the center alignment

Figure 5. Stator recognition procedure

3.1. *Keypoint matching*

Keypoint matching requires two images which are template and target images. The method detects a portion of the target image, which is similar to the template image.

Keypoints are extracted from the images. The keypoints are robust to translation, rotation, scaling, and brightness changes. The details of the Keypoint matching are shown in [7]. To calculate the similarity, we use Hamming distance. If both character strings are represented as α and β, the Hamming distance $\mathrm{Ham}(\alpha,\beta)$ is represented by

$$\mathrm{Ham}(\alpha,\beta) \coloneqq \sum_{i=1}^{m} \begin{cases} 1 & (\alpha[i] \neq \beta[i]) \\ 0 & (\alpha[i] = \beta[i]) \end{cases} \tag{1}$$

From each of the template and target images, we extract the top k key points with the highest similarity among the feature points. The points are matched as shown in Figure 6. This is called K-Nearest Neighbor matching. A 2 by 3 affine transformation matrix is estimated by RANSAC. The orientation of the stator is then obtained from the following three points: The center coordinate of the bounding rectangle of the similar portion of the target image, and the upper left vertex coordinates before and after affine reconstruction (Figure 7).

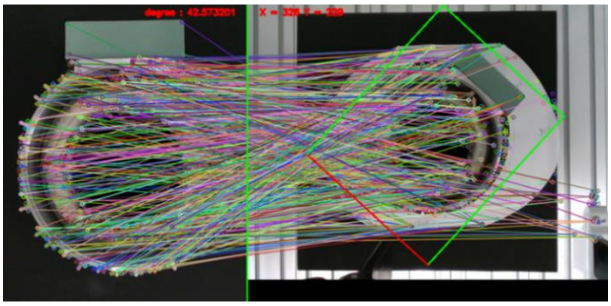

(a) Template image (b) Target image

Figure 6. Keypoint matching

(a) Template image (b) Target image

Figure 7. Orientation detection

3.2. *Contact position estimation*

Since the stator insertion is not always smooth, the appropriate insertion motion must be generated. For this purpose, the contact position between the stator and the rotor is detected by the force torque sensor information. While the stator is inserted, the contact position is detected and corrective action avoiding the contact position is generated repeatedly.

From the 6-axis force torque sensor, force and moment measurements $(\boldsymbol{f}_i, \boldsymbol{m}_i)$ are acquired, in which the subscript i denotes $1,2,\cdots,k$. Deviation data $(\bar{\boldsymbol{f}}_i, \bar{\boldsymbol{m}}_i)$ from the average are computed to eliminate the offset of the data. Let $\boldsymbol{p}_c$ be the position of the contact point, the formula $\boldsymbol{p}_c \times \bar{\boldsymbol{f}}_i = \bar{\boldsymbol{m}}_i$ is obtained in pure case. In practical case, the measurements are contaminated with noise, then we define the following evaluation function:

$$J(\boldsymbol{p}_c) := \frac{1}{k}\sum_{i=1}^{k} \left\| \bar{\boldsymbol{m}}_i - \boldsymbol{p}_c \times \bar{\boldsymbol{f}}_i \right\|^2 \tag{2}$$

The function is minimized, then the estimate of the position is obtained by the following formula:

$$\hat{\boldsymbol{p}}_c := \left(\frac{1}{k}\sum_{i=1}^{k} [\bar{\boldsymbol{f}}_i \times]^2\right)^{-1} \left(\frac{1}{k}\sum_{i=1}^{k} \bar{\boldsymbol{m}}_i \times \bar{\boldsymbol{f}}_i\right) \tag{3}$$

The minimum value is calculated by $s_k := J(\hat{\boldsymbol{p}}_c)$. We obtain an uncertainty region of the estimate $\hat{\boldsymbol{p}}_c$ by

$$J(\boldsymbol{p}_c) \leq 2s_k \tag{4}$$

The region generates an ellipsoid centered at the estimate. The derivation of the region is explained in [8]..

4. Experiments

4.1. *Procedure of experiments*

To verify our proposed system, the following steps is performed.

Step 1. Detect the position of the stator, in which the Hough transform is applied as explained in Section 3.

Step 2. Detect the orientation of the stator, in which the Key point matching is applied as explained in Section 3.1..

Step 3. The robot arm moves just above the stator (Figure 8) and the hand grasps it. The stator is lifted and moved just above the rotor and reducer (Figure 9).

Step 4. The insertion operation is performed. If the stator meets the rotor, the corrective motion is generated till the proper insertion position is reached.

Step 5. Once the stator reaches and places the proper position, the insertion motion is terminated.

Figure 10 shows the details of **Steps 4** and **5**. During no contact is detected in **Step 4**, the stator is lowered. If the contact is detected, the stator is raised 3 mm in z component (vertical component) and moved 1 mm in the x and y components (horizontal components) to avoid and break a jamming. The x and y components are given along the direction of the detected contact position.

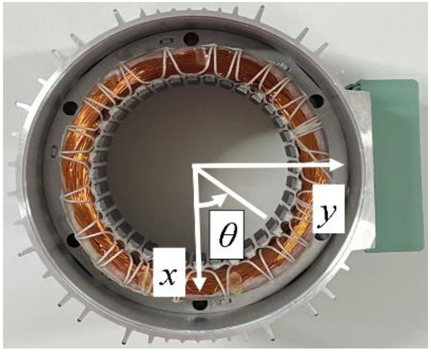

Figure 8. Contact position direction in the stator coordinates

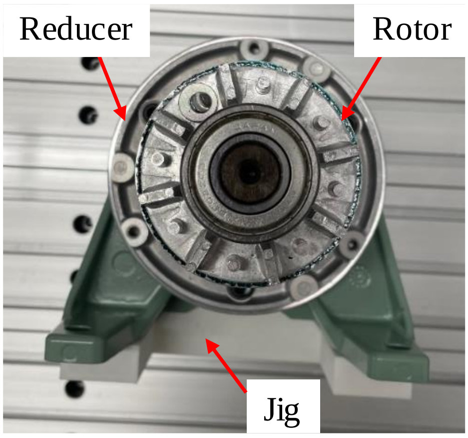

Figure 9. Top view of the reducer with the rotor

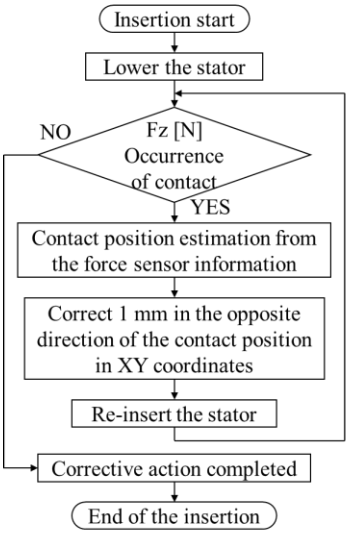

Figure 10. Flowchart of the insertion process

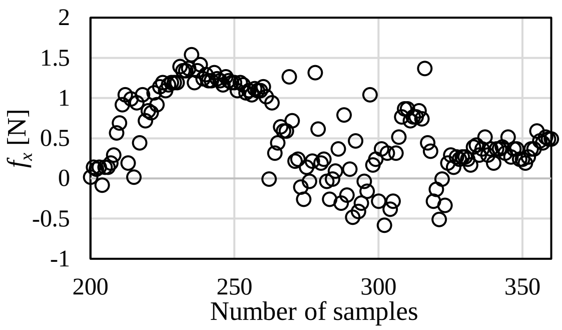

(a) f_x component

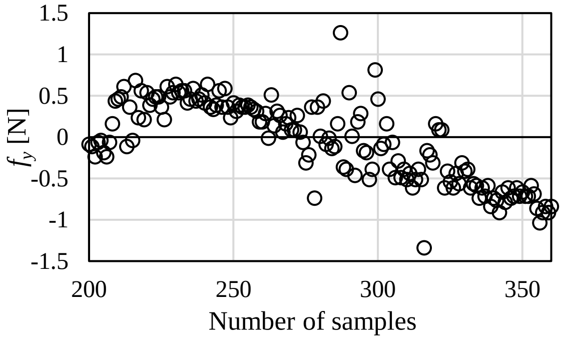

(b) f_y component

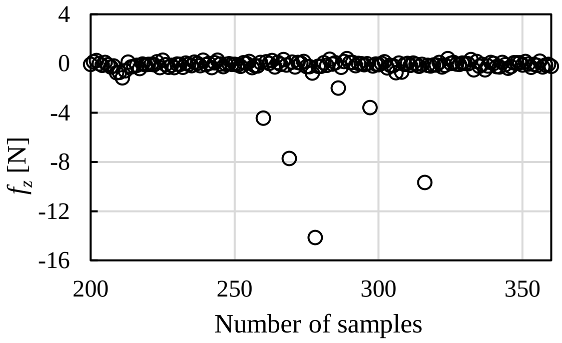

(c) f_z component

Figure 11. Measurement force

Success condition: After the insertion operation of the stator, we check manually whether the bolts can go through both bolt holes of the stator and reducer.

Number of trials: 10 trials for each of the following 8 shift conditions, 80 trials in total. The 8 shift conditions mean that the stator position is somewhat shifted to the directions (0°, 45°, 90°, 135°, 180°, 225°, 270°, 315°) which are viewed in the robot coordinates. This means that the stator meets the rotor when the insertion operation is performed. Figure 8 shows the robot coordinates (x, y) and its angular orientation θ on the stator. In the experiments, we set the initial condition as that the stator is shifted beforehand about 2 mm from the nominal aligned position.

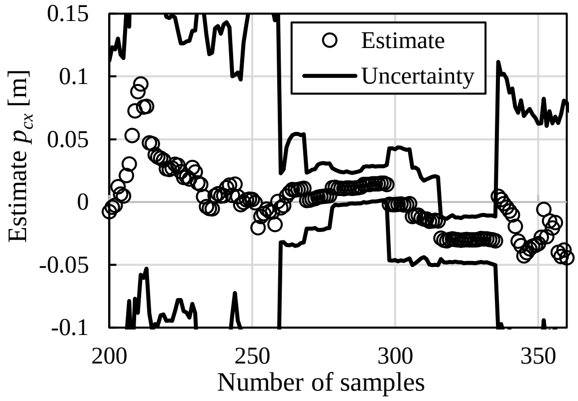

(a) X component $\hat{p}_{cx}$

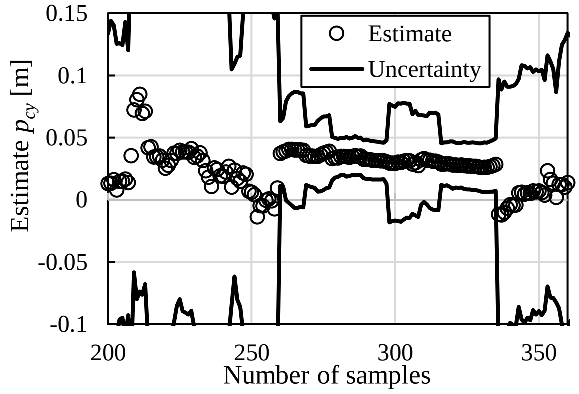

(b) Y component $\hat{p}_{cy}$

Figure 12. Estimates of the position of contact point and its uncertainty

4.2. *Results of the experiments*

Figure 11 shows the force torque measurements. Moment components are omitted for the page space. Figure 12 shows the x-y components of the estimate $\hat{\boldsymbol{p}}_c$ and its uncertainty. These figures show that the angle of the preset contact direction is the case of 90°. The sampling time of the force torque sensor is 18.6 msec. The last 20 data, $k = 20$, are used in Eq. (3). As seen in Figure 12, the contact repeatedly appears in the samples from 226 to 316. When the uncertainty gets narrow, the estimate is valid. In Figure 11 and 12, we focus on the valid range of estimation.

As shown in Figure 11, the contact forces widely fluctuate when the stator meets the rotor. The force torque measurements will be zeros in ideal cases with no contacts, however, slightly fluctuate with noise and some others in real cases. The data fluctuation also occurs due that the force torque sensor slightly sways by the robot motion.

Since the rotor diameter is about 70 mm, the position of the nominal contact point occurs on about 35 mm radius in x-y components. From Figure 12, the position is estimated on about 35 mm radius. The nominal contact point remains inside the area calculated by the estimated contact position and its uncertainty. The estimated position shifts from about 0.0 mm to -30.8 mm in the $\hat{p}_{cx}$ component (Figure 12(a)) and from about $+37.2$ mm to $+28.3$ mm in the $\hat{p}_{cy}$ component (Figure 12(b)). The angle of the contact direction is calculated by the formula $\hat{\theta} = \mathrm{atan2}(\hat{p}_{cy}, \hat{p}_{cx})$. The angle shifts from about $+90°$ to $+137°$. Based on the estimated angle, the corrective motion of the robot is generated. After the motion, the contact disappears, and the insertion motion is accomplished.

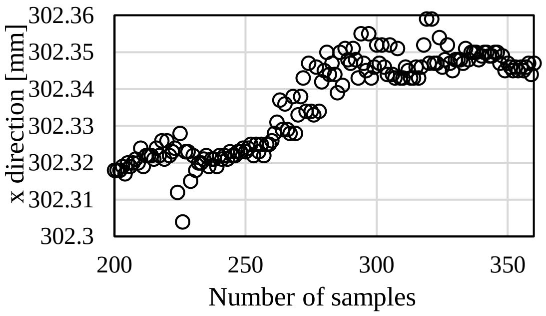

(a) Motion in the x direction

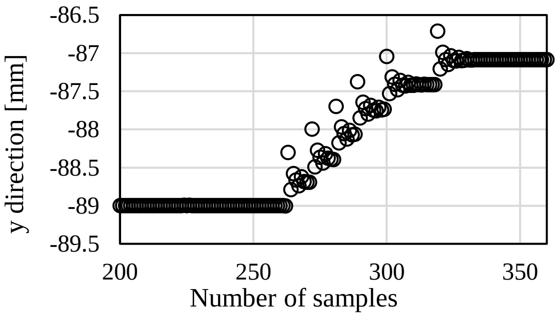

(b) Motion in the y direction

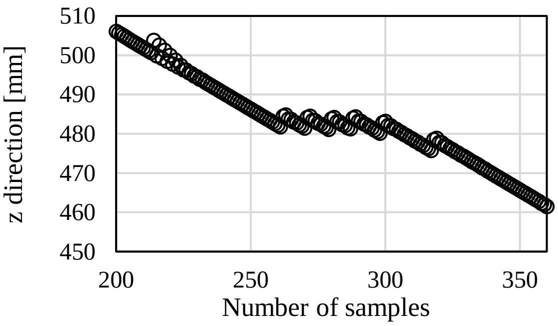

(c) Motion in the z direction

Figure 13. Translation direction of the insertion motion

If a threshold is set for the magnitude of the contact force to distinguish whether the contact occurs or not, we can omit the plots of the estimates in the invalid samples ([200, 225] and [317, 320]). For readers understanding, we plotted the estimated contact position obtained by Eq. (3) in the invalid samples with no contacts.

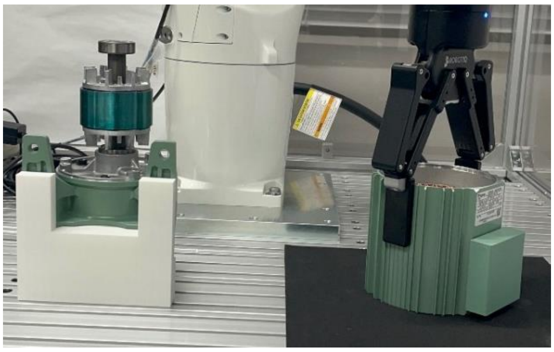

(a) The reducer with the rotor, and the stator grasped by the robot hand

(b) The stator moved just above the reducer (Step 3)

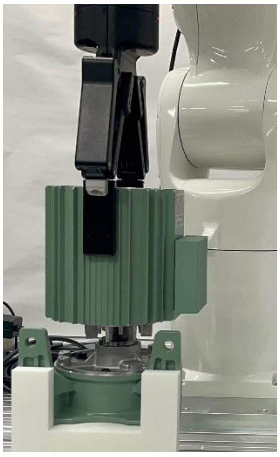

(c) The stator insertion motion (Step 4)

(d) Completion of the insertion

Figure 14. Steps of the insertion process

Figure 13 shows the corrective motion of the robot arm. The robot detects the contact between the stator and the rotor by the force information, performs corrective motion in the x and y directions (Figure 13(a), (b)), and lower the position in the z direction (Figure 13(c)) gradually. From the viewpoint of the robot coordinates, the x component shift from about 302.32 mm to 302.34 mm in which the component shifts about +0.02 mm (Figure 13(a)), the y component shifts from about -89.0 mm to -87 mm in which the component shifts about +2 mm (Figure 13(b)). In the z component, the stator meets the rotor many times about 480 mm, the corrective motion is generated slightly, and the robot makes lowering motion. After that, the contact between the stator and rotor disappears, the stator is approached to the reducer, and the placing of the stator is accomplished (Figure 13(c)). Figure 14 shows photos of the insertion sequence. Figure 14(a) shows the phase that the stator is grasped by the robot hand after the pose recognition of the stator using the image sensor. The grasped stator will be inserted to the rotor shown in the left side. Figure 14(b) shows the phase that the stator is moved just above the rotor. Figure 14(c) shows the phase that the stator is just inserted to the rotor using the corrective motion. Figure 14(d) shows the phase that the insertion motion is completed.

Table 1 shows the results of the success rate, the average time of the corrective motion, and the average time of the insertion motion. Experimental success rate was 100 % in all conditions. It took about 70 and 170 seconds to perform the corrective motion and the insertion, respectively. Due to the early development stage in this paper, the robot speed was limited to 2 % of the maximum speed. For this reason, we took the long motion times to complete the insertion tasks.

As described in "Success condition" and " Number of trials " in Section 4.1, the success rate means that the stator successfully mated the reducer in all of the 10 trials for each contact direction.

Table 1. Average time of the insertion motion

Contact direction [deg]	Success rate [%]	Average time of the correction motion [sec]	Average time of the insertion [sec]
0	100	69.6	171.9
45	100	83.7	193.1
90	100	64.7	171.2
135	100	68.5	174.1
180	100	78.7	181.8
225	100	69.4	171.9
270	100	72.8	178.1
315	100	67.8	171.4

5. Conclusions

This paper tackled the robotic assembly of the gearmotor. In the process, the stator was recognized by Hough transform and Keypoint matching using visual sensation and then inserted into the rotor and reducer by using the contact position estimation from the force torque information. The validity of our method was verified by the experiments. In the experiments, we achieved 100 % in the success rate of the insertion. To shorten the insertion of the experiments, we will try to improve the measurements and insertion process in our future work.

In this paper, we discussed the stator insertion process only. In our future work, we will attack assembly processes of all the parts of gearmotors.

References

1. J. E.C. Mateus, E.-H. Aghezzaf, D.Claeys, V. Lemère, J. Cottyn, Method for transition from manual assembly to Human-Robot collaborative assembly, IFAC PaperOnLine, Vol. 51, No. 11, pp. 405-410, 2018.
2. R. Gervasi, m. Capponi, L. Mastrogiacomo, F. Franceschini, Manual assembly and Human-Robot Collaboration in repetitive assembly processes: a structured comparison based on human-centered performances, Int. J. Advanced Manufacturing Technology, Vol. 126, pp. 1213-1231, 2023.
3. O. Salunkhe, O. Stonsöta, M. Åkerman, Å. F. Berglund, P.-A. Alveflo, Assembly 4.0: Wheel Hub Nut Assembly Using a Cobot, IFAC-PapersOnLine Vol. 52, No. 13, pp. 1532-1637, 2019.
4. Y. Ma, K. Du, D. Zhou, J. Zhang, X. Liu, D. Xu, Automatic precision robot assembly system with microscopic vision and force sensor, Int. J. of Advanced Robotic Systems, May-June 2019, pp. 1-15, DOI: 10.1177/1729881419851619.
5. R. Song, F. Li, W. Quan, X. Yang, J. Zhao, Skill learning for robotic assembly based on visual perspectives and force sensing, Robotics and Autonomous Systems, Elsevier, Vol. 135, 103651, 2021.
6. Wen-Chung Chang, Robotic assembly of smartphone back shells with eye-in-hand visual servoing, Robotics and Computer-integrated Manufacturing, Elsevier, Vol. 50, pp. 102-113, 2018.
7. P. F. Alcantarilla, J. Nuevo, A. Bartoli, Fast Explicit Diffusion for Accelerated Features in Nonlinear Scale Spaces, Proceedings of British Machine Vision Conference (BMVC), pp. 1-11, 2013.
8. T. Yamada, A. Tanaka, M. Yamada, Y. Funahashi, H.Yamamoto, Identification of Contact Conditions by Active Force Sensing (Estimated Parameter Uncertainty and Experimental Verification), J. of Robotics and Mechatronics (JRM), Vol. 23, No. 1, pp. 44-52, 2011.

Authors Introduction

Dr. Takayoshi Yamada.

He is a Professor with the Department of Mechanical Engineering, Gifu University. He received the B.E., M.E, Ph.D. degrees in Mechanical Engineering from the Nagoya Institute of Technology, Japan, in 1991, 1993, 1995, respectively. He is a member of the Japan Society of Mechanical Engineers (JSME), the Robotics Society of Japan (RSJ), the Society of Instrument and Control Engineers (SICE) , IEEE, and the Japan Society of Precision Engineering (JSPE). His research interests include grasping, manipulation, sensing, and automation systems.

Mr. Yasumoto Imai.

He is a member of the staff of Mitsubishi Electric Corporation in Japan. He received the B.E. and M.E. degrees in Mechanical Engineering from Gifu University, Japan, in 2021 and 2023, respectively.

Dr. Junya Sato.

He is an Assistant Professor with the Department of Mechanical Engineering, Faculty of Engineering, Gifu University, Japan. He received the B.E., M.E., and Ph.D. degrees in Engineering from Iwate University in Japan, in 2012, 2014, and 2017, respectively. He is a member of the IEEE, the institute of Electrical Engineers of Japan (IEEJ), the Japanese Academy of Facial Studies (JFACE), and JSPE. His research interests include applications of evolutionary computations to computer vision.

Mr. Toshiki Hayashi.

He is a member of the staff of Tsubakimoto Chain Co. in Japan. He received the B.E. degree in Mechanical Engineering from Kanazawa Institute of Technology, Japan, in 2013. His research interests include robotic assembly and human-robot collaboration.

Mr. Shota Aono.

He is a member of the staff of Tsubakimoto Chain Co. in Japan. He received the B.E. degree in Electronics from Doshisha University, Japan, in 2018. His research interests include robotic assembly and human-robot collaboration.